# Fiber-Optic Sensing and CNN-LSTM Time-Series Model with Dynamic Path Generation for Coal-Mine Ventilation Wind-Speed Prediction

Kangning Dong<sup>1\*</sup>, Lei Wang<sup>2</sup>

1\*College of Mechanical Engineering, University of Science and Technology Beijing, Beijing 100083, China

<sup>2</sup>Coal Mine ventilation Department, Zhaogu No. 1 Coal Mine, Xinxiang City 453634, China

E-mail: dongkn04@163.com

Keywords: coal mine ventilation, fiber optic sensing, time series prediction, deep learning

Received: August 26, 2025

This article proposes a time-series prediction algorithm model based on fiber optic sensing and deep learning to address the problem of insufficient accuracy in wind speed monitoring and prediction of coal mine ventilation systems under complex working conditions. We have developed a mechanism for fiber optic deployment and signal transmission, designed a real-time monitoring and data acquisition platform, and achieved structured processing of mine wind speed data through feature extraction. At the model level, an improved long short-term memory network and convolutional neural network fusion prediction framework are introduced to model wind speed time series, and combined with dynamic prediction path generation algorithm to enhance prediction robustness. The model forecasts 12 hours ahead using 24-hour inputs, with three CNN layers, two LSTM layers, and attention. The experiment used 120-day data from 48 fiber-optic sensors at 20 Hz, yielding  $1.2 \times 10^8$  records plus 950k equipment samples and 17k event logs. After anomaly correction and normalization preprocessing, traditional ARIMA, BP neural network models were compared using metrics such as root mean square error, mean absolute error, and coefficient of determination ( $R^2$ ). Training used a 70/20/10 split with Adam (Ir = 0.001, batch = 64); results averaged over 30 runs significantly outperformed ARIMA and BP (p < 0.01). Results showed MAE 0.18 m/s (95% CI: 0.16-0.20), RMSE 0.23 (95% CI: 0.21-0.26), R<sup>2</sup> 0.94 (95% CI: 0.92-0.95), and delay 1.2 s (95% CI: 1.1-1.3), confirming robustness under complex conditions. The ablation experiment further validated the contribution of feature extraction and dynamic path module to overall performance. The research conclusion shows that the model can effectively improve the wind speed monitoring and prediction level of coal mine ventilation systems, and provide a feasible technical path for intelligent scheduling and safety warning. The results are based on field-deployed data, with 95% confidence intervals reported for all metrics.

Povzetek: Za prezračevanjenje v jamah je razvit integriran sistem optičnovlakenskega merjenja in globokega učenja (CNN–LSTM z dinamično generacijo poti) za 12-urno napoved hitrosti zraka, ki na realnih podatkih pomembno zmanjša pogreške, zakasnitev in omogoča zanesljivejše delovanje.

#### 1 Introduction

Coal mine ventilation systems are vital for safety and efficiency. As mining depths increase, traditional monitoring methods struggle with real-time performance, accuracy, and robustness. Wind speed, a key parameter, is affected by factors like tunnel structure and fan load, causing fluctuations and noise that complicate prediction and scheduling. Electrical anemometers fail to meet the needs of high-frequency sampling, leading to unreliable data for intelligent scheduling and safety.

Fiber optic sensing technology has become crucial for monitoring mine wind speed due to its resistance to interference, distributed measurement, and adaptability. While it provides real-time data, predicting wind speed remains a challenge due to its nonlinear and non-stationary nature. Deep learning models, such as LSTM and CNN, can improve accuracy by 10%-20% over traditional methods,

supporting a "monitoring, prediction, scheduling" framework.

This paper proposes a time series prediction model using fiber optic sensing and deep learning, combining data acquisition, dynamic feature extraction, and intelligent prediction with scheduling. The model includes: (1) sensor deployment and signal transmission, (2) predictive algorithms and dynamic path optimization, and (3) collaborative operation. Compared to traditional methods, this framework offers real-time, adaptive feedback and robustness under various conditions.

Unlike static curve fitting or local parameter tuning, this method integrates real-time data, prediction, and path generation, achieving faster responses under disturbances. The proposed method improves prediction accuracy and reduces response delay, providing an optimized path for intelligent mine ventilation systems.

The experimental part is based on the measured wind speed dataset, using metrics such as root mean square error,

mean absolute error, and coefficient of determination (R²) to compare with models such as ARIMA and BP neural network. The contribution of the module is verified through ablation experiments. This study uses ARIMA and BP neural networks as baselines. For ARIMA, order selection was based on AIC/BIC, with first-order differencing and seasonal components. For BP, the model had one hidden layer of 64 units, trained for 200 epochs with a batch size of 32 using Adam (lr = 0.001). Hyperparameters were tuned via grid search, with early stopping after 10 epochs. All models were evaluated with 5-fold cross-validation. The research objective is to construct an intelligent prediction scheme with real-time, robustness, and scalability, providing technical support for the safety warning and optimization scheduling of coal mine ventilation systems.

#### 2 Related work

Coal mine ventilation systems are critical for safety, traditionally relying on fixed measuring points and static models for long-term wind speed monitoring and prediction. While these methods are reliable in stable conditions, they suffer from prediction delays, poor abnormal response, and low resolution in complex, high-load environments. Statistical methods, such as curve regression, handle only stationary time series and struggle with nonlinear fluctuations. ARIMA and similar models are

prone to overfitting and lack generalization when processing large-scale, multi-source data, limiting their effectiveness in disaster warning and intelligent scheduling.

In recent years, fiber optic sensing has proven advantageous for ventilation monitoring. Wang et al. (2024) proposed a denoising method based on CEEMDAN and wavelet thresholding, outperforming traditional methods in short-term prediction but with high computational cost in multi-channel scenarios [1]. Shen et al. (2022) developed a low-power ventilation wind speed monitoring device using vortex-excited frictional nanogenerators, offering real-time monitoring in high-frequency disturbances [2]. Li et al. (2021) achieved continuous underground wind speed sensing through temperature-compensated fiber optic gas flow sensors, overcoming fixed-point limitations. However, their single fitting algorithm struggles with global prediction needs [3]. Sheng Xiang and Lin's (2022) hybrid deep learning framework, combined with time series decomposition and multi-objective optimization, improves accuracy but still faces delays in high-disturbance environments [4].

To highlight the differences between traditional methods and deep prediction models, this study summarizes the comparison of existing coal mine ventilation wind speed monitoring and prediction methods in terms of data acquisition, feature modeling, prediction framework, abnormal response, etc., as shown in Table 1.

Table 1: Comparison of representative methods for coal-mine ventilation wind-speed prediction (MAE/RMSE in m/s,
latency in s, R unitless)

Study	Data	Method	MAE	RMSE	R	Latency	Limitation
Wang et al. (2024) [1]	Fiber signals	CEEMDAN+WT	0.35	0.48	0.85	>3.0	No scheduling, costly
Shen et al. (2022) [2]	TENG sensor	Regression	0.42	0.55	0.81	2.8	Low robustness
Li et al. (2021) [3]	FBG gas- flow	Regression	0.31	0.45	0.87	3.5	Monitoring only
Sheng-Xiang & Lin (2022) [4]	Wind series	Hybrid DL	0.26	0.33	0.90	2.6	No scheduling
Zhao (2024) [5]	Gas emission	SSA-LSTM	0.24	0.30	0.91	2.4	No monitoring loop
Yuan et al. (2025) [9]	Gas conc.	DL- Koopman+PID	0.22	0.29	0.92	2.2	Gas-focused
This study	48 FBG, 120 d	CNN– LSTM+Path	0.18	0.23	0.94	1.2	Full integration

From Table 1, traditional statistical methods show lower computational cost but exhibit large errors (MAE 0.31-0.42 m/s, RMSE 0.45-0.55, R  $\leq 0.87$ ) and high latency (>3.0 s), limiting their adaptability under dynamic ventilation conditions. Deep learning approaches improve accuracy (MAE 0.22-0.26, RMSE 0.29-0.33, R up to 0.92), yet still suffer from delays of 2.2-2.6 s and lack integration with real-time scheduling. Achieving both high-resolution prediction and low-latency response therefore remains the core challenge in coal-mine ventilation research.

Recent studies have explored the integration of fiber optic sensing and deep prediction frameworks. Zhao (2024) proposed a time series prediction method for coal mine gas emissions using optimized variational mode decomposition

and SSA-LSTM, showing strong robustness under disturbances [5]. Meng et al. (2022) combined deep learning with classical time series analysis for methane concentration prediction, demonstrating improved stability with multi-source sensor inputs, though dynamic scheduling remained a challenge [6]. Lim and Zohar (2021) highlighted the shift from single-step to multi-step dynamic prediction in deep learning, offering new insights for modeling ventilation wind speed [7].

Existing research shows that coal mine ventilation wind speed prediction is moving from "static fitting" to "dynamic learning," yet lacks a comprehensive architecture for real-time monitoring, deep prediction, and dynamic scheduling. The proposed integrated framework combines

fiber optic sensor deployment, data feature extraction, CNN-LSTM fusion prediction, and dynamic path generation. It achieves low latency and high-precision predictions under disturbances and demonstrates strong scalability. This study's innovation lies in: 1) achieving a closed-loop linkage of monitoring, prediction, and scheduling; 2) improved stability and deployability under complex conditions; and 3) compatibility with Python and AnyLogic for cross-platform testing. This framework not only offers a new path for mine wind speed monitoring and prediction but also supports the development of intelligent ventilation scheduling systems.

## 3 Design of fiber optic wind speed monitoring system

## 3.1 Layout and signal transmission of fiber optic sensors

There is a common problem of lagging wind speed monitoring and scheduling, as well as delayed response of prediction strategies in coal mine ventilation systems, especially in the deployment of multi node sensors and heterogeneous data exchange processes, which can easily lead to imbalanced task and resource matching and ineffective control strategies. This article introduces the modeling of the "task node scheduling" ternary relationship in the deployment scheme of fiber optic sensors, focusing on solving the problems of uneven transmission paths of wind speed data and lagging monitoring instructions. Simulate and optimize the wind speed sensing task and signal transmission link through modular modeling, and verify the advantages and disadvantages of the model in terms of execution delay and system response through comparative experiments. Sensor calibration performed with reference anemometers before deployment. Fiber loss coefficient  $\gamma$ =0.23 dB/km, cable attenuation assumed 0.19 dB/km, PCA retained 95% variance.

To ensure the reproducibility of the research, this paper adopts a multi-agent simulation method to model the fiber optic monitoring nodes, transmission links, ventilation dispatch center servers, and edge gateways in coal mine tunnels as independent modules. Build a dynamic running model on the AnyLogic 8.7 platform and set different categories of wind speed monitoring tasks and fiber channel allocation rules, so that the simulation focuses on event triggering (such as sudden wind speed changes) and link state changes (such as channel congestion). The signal transmission adopts an improved A \* algorithm for optimal fiber path search, combined with load balancing strategy to reduce node overload risk. The system interaction layer implements real-time push of wind speed data through WebSocket and Kafka, and the backend uses Python and Flask interfaces to issue ventilation control commands and collect transmission status. The evaluation indicators cover transmission latency, data packet loss rate, and channel utilization, and the effectiveness of key mechanisms is analyzed through ablation experiments.

The research process is as follows: ①Using AnyLogic 8.7 as the modeling environment, modular construction is

carried out on fiber optic sensor nodes, transmission channels, and ventilation schedulers;(2)Set task category  $T = \{t_1, t_2, \dots, t_n\}$ and allocation  $R = \{r_1, r_2, \dots, r_n\}$ , with wind speed sudden change events and link state changes as triggering conditions; (3) Adopting an improved A \* search combined with load priority strategy to generate dynamic fiber optic transmission paths; 4) Use WebSocket and Kafka to exchange wind speed monitoring data messages, and Python and Flask to synchronize control instructions and status; (5) Compare different scheduling schemes using transmission delay L, packet loss rate P, and utilization rate U as performance indicators; (6) Remove the path optimization and load balancing modules through ablation experiments to test the role of each mechanism in overall performance improvement.

The deployment process of fiber optic sensors needs to consider the node distribution density and signal attenuation characteristics. If the length of the mine ventilation section is L, the set of fiber optic sensor nodes is  $S = \left\{s_1, s_2, \ldots, s_n\right\}$ , and each node corresponds to a deployment position of  $P_i$ , then the optimal deployment problem can be formalized as:

$$\min J = \sum_{i=1}^{n} \left[ \alpha \cdot d(p_i, p_i + 1) + \beta \cdot A(p_i) \right]$$
(1)

Among them,  $d(p_i,p_i+1)$  represents the spatial distance between adjacent nodes,  $A(p_i)$  represents the variance of wind speed fluctuations at nodes, and  $\alpha$ ,  $\beta$  is the weight coefficient. This optimization function ensures that the deployment covers both high disturbance areas and transmission signal strength, thereby reducing global monitoring errors.

In terms of signal transmission, this article adopts a combination of wavelength division multiplexing and time division multiplexing to decouple the reflected signals of different nodes in frequency spectrum, achieving multipoint synchronous acquisition. Assuming the transmission signal is E(t), the signal strength after propagation through optical fiber can be expressed as:

$$I(t) = I_0 \cdot e^{-\gamma L} \cdot \cos^2\left(\frac{\pi \Delta nL}{\lambda}\right)$$
 (2)

Among them, where  $I_0$  is the initial signal intensity,  $\gamma$  is the fiber loss coefficient,  $\Delta n$  is the refractive index difference, and  $\lambda$  is the wavelength of the incident light. This transmission model ensures that signals can still be maintained within a recognizable signal-to-noise ratio range in complex mine channels over 5km.

In order to adapt to the dynamic characteristics of the ventilation system, the signal transmission architecture is designed as a hierarchical model of edge computing+cloud training. Set a edge computing node near the mine working face to complete real-time demodulation, feature extraction and anomaly detection, and transmit it to the cloud central server through WebSocket protocol to achieve second level feedback. Experimental verification shows that edge nodes can control the average response time within 0.8s in delay control, which is about 57% shorter than the delay of a single cloud architecture.

In addition, fiber optic sensing signals are susceptible to interference from mining and mechanical vibrations during transmission. This article introduces the denoising mechanism of wavelet packet decomposition+principal component analysis to denoise and enhance the features of

the original signal. Assuming the original signal xt(t) is decomposed into multiple components  $\{x_1(t), x_2(t), \ldots, x_m(t)\}$ , and then the main component y(t) is selected through PCA, the reconstructed signal satisfies:

$$y(t) = \sum_{j=1}^{k} w_j x_j(t)$$
(3)

Experiments have shown that this noise reduction mechanism can improve signal stability by about 21.6% in mine wind speed monitoring, effectively suppressing false alarms caused by local disturbances.

At the system implementation level, the logical information layer of this article is based on MySQL database and Flask interface to complete model parameter management and data entry; The physical layer collects wind speed data through fiber optic deployment and OPC-UA protocol to ensure accuracy and universality; The interactive mapping layer utilizes Node RED for data flow and visualization, and cross platform integration is achieved between layers through RESTful APIs. To ensure time consistency, signals were sampled at 20 Hz and aligned with 5-s timestamp anchors for multi-source synchronization."

To ensure reproducibility, detailed simulation settings of AnyLogic 8.7 are provided. The agent layer consists of sensor nodes, transmission channels, and scheduling servers. Sensor agents generate wind speed events with a Poisson distribution ( $\lambda$ =0.15), and transmission delays follow an exponential distribution (mean=2.5s). The improved A\* algorithm applies a load-priority cost function :

$$C = d + \alpha l + \beta b^{-1} \tag{4}$$

where d is distance, l is node load, and b is bandwidth. Appendix A includes parameter tables and agent diagrams, with model files supplied for replication. This ensures reproducibility and highlights the stability and scalability of the scheme under complex conditions, providing high-quality input for time-series prediction.

The pseudocode for the improved A\* path finder, including its complexity and parameters, is provided:

Input: SensorData, NodeStatus For each packet in SensorData:

Extract features = f(packet.signal)

Compute cost = C(sensor, candidate\_node)

Select target\_node = argmin(cost)

Assign packet to target\_node

Update NodeStatus

End For

This pseudocode outlines the packet processing steps: feature extraction, cost calculation, node selection, and state updates.

## 3.2 Data collection and real time monitoring platform architecture

The real-time and reliable monitoring of wind speed in coal mine ventilation systems is a key factor in ensuring mine safety in complex tunnel networks and multi-source interference environments. Traditional monitoring methods rely heavily on fixed point sensors and centralized data collection, which suffer from high response latency, untimely anomaly detection, and insufficient system scalability. To address these bottlenecks, this article constructs a real-time monitoring platform architecture based on fiber optic sensing, which achieves continuous monitoring and dynamic scheduling of wind speed signals through distributed node deployment, data flow management, and prediction driven task collaboration.

In platform design, each fiber optic monitoring node is abstracted as an independent unit that includes signal input, task triggering, resource binding, and status feedback. The node status is synchronized in real-time by a digital twin module, ensuring that the system has dynamic reconfigurability under multi-source data streams. The overall architecture of the system is shown in Figure 2, including the sensing layer, communication layer, scheduling layer, and prediction layer. Among them, the sensing layer completes the collection and preliminary filtering of wind speed signals, the communication layer achieves high-speed transmission based on fiber edge gateway links, the scheduling layer allocates paths and provides abnormal feedback through task engines, and the prediction layer embeds time series models to calculate future wind speed trends.

In order to ensure the optimality of scheduling, this paper introduces an improved cost function in the scheduling layer to optimize the allocation strategy of task nodes. The cost function is defined as follows:

$$C(i,j) = \alpha \cdot d(i,j) + \beta \cdot l(j) + \gamma \cdot \frac{1}{A(j)}$$
(5)

Among them, d(i,j) represents the transmission distance between monitoring point i and computing node j, l(j) represents the current load level of the node, and A(j) represents the available bandwidth of the node;  $\alpha$ ,  $\beta$ ,  $\gamma$  is the weight coefficient, and parameter calibration is carried out through experiments. This function can comprehensively consider distance overhead, load pressure, and resource utilization to achieve dynamic

optimal allocation of wind speed monitoring tasks in complex mine topologies.

At the implementation level, the data collection and task scheduling process is expressed in pseudocode as follows:

Input: SensorData, NodeStatusFor each packet in SensorData:

Extract features = f(packet.signal)

Compute cost = C(sensor, candidate\_node)

Select target\_node = argmin(cost)

Assign packet to target\_node

Update NodeStatusEnd For

This process ensures balanced allocation of data streams in the transmission link, while avoiding delays and packet loss caused by node congestion.

The platform introduces a sliding monitoring window mechanism during operation to perform real-time detection of sudden changes in wind speed, link blockage, and transmission errors. When an abnormal event is triggered, the scheduling engine will regenerate the path based on the current state graph and notify the prediction module to complete the model update through the feedback channel. In this way, the system has adaptive adjustment and dynamic fault tolerance capabilities, maintaining high efficiency and stability under complex working conditions.

To enhance the reproducibility of the platform, this study uses Python to implement data scheduling logic and constructs dynamic simulation scenarios in AnyLogic 8.7 to achieve visual verification of the entire wind speed collection, transmission, and prediction chain. The system completes data stream interaction with Kafka through WebSocket, and the Flask interface provides control instructions to synchronize with predicted results. In the experimental environment, the platform can achieve millisecond level delay control and a data integrity rate of over 98%, significantly better than traditional centralized monitoring architectures.

## 3.3 Feature extraction and structured processing of fiber optic monitoring data

The wind speed monitoring data in the coal mine ventilation system has the characteristics of strong temporal variability, multiple noise interferences, and complex multi-source coupling. If relying solely on single point data or static threshold determination, it is difficult to support the construction of subsequent time-series prediction models. Therefore, this study proposes a feature extraction and structured processing framework based on fiber optic monitoring data, which realizes the systematic transformation from raw signals to computable features,

ensuring that the model input has interpretability and predictive driving ability.

The settings for FFT window length, wavelet packet configuration, PCA variance threshold, and mutual information feature selection are provided:FFT Window Length: 128 points, Hamming window.Wavelet Packet: Daubechies-4, 3 levels.PCA Threshold: 95% variance.Mutual Information Threshold: MI > 0.05.

At the data input layer, fiber optic deployment nodes transmit wind speed disturbance signals to the monitoring platform in a distributed manner, forming a multidimensional temporal matrix. The raw data was segmented into 60-s windows and denoised using Daubechies-4 wavelet packet decomposition (3 levels). PCA (95% variance) and FFT with a Hamming window extracted temporal and spectral features, complemented by statistical descriptors. Mutual information (MI > 0.05) guided selection of 12 final features, including wind speed mean, fluctuation amplitude, turbulence intensity, FFT peak frequency/bandwidth, entropy, skewness, kurtosis, temperature, humidity, tunnel position, and sensor ID. The formula is as follows:

$$F_{t} = \frac{1}{n} \sum_{i=1}^{n} (x_{t+i} - \mu)^{2}$$
(6)

Among them,  $F_t$  represents the feature variance within the time window,  $x_{t+i}$  is the monitoring value within the window, and  $\mu$  is the mean wind speed within the time window. This process ensures that abnormal wind speed fluctuations are amplified at the feature level, making it easier for predictive models to identify.

In the structured representation stage, all features are uniformly mapped to a tensor representation matrix, and a three-dimensional feature cube is constructed by combining timestamps, spatial positions, and sensor numbers. This structure enables the system to simultaneously capture vertical temporal dependencies, horizontal spatial correlations, and cross dimensional feature interactions, significantly enhancing its modeling capabilities for complex ventilation environments in mines. To further enhance real-time performance, this study introduces a streaming computing framework in the feature processing module, which updates the feature extraction results synchronously with the prediction module in milliseconds through a data bus. Once abnormal disturbance is detected (such as sudden drop of wind speed in a certain section), the characteristic flow will immediately trigger the abnormal mark, and adjust its weight in the next round of prediction input to avoid prediction distortion due to abnormal data diffusion. The entire process of feature extraction and structuring is shown in Figure 1.

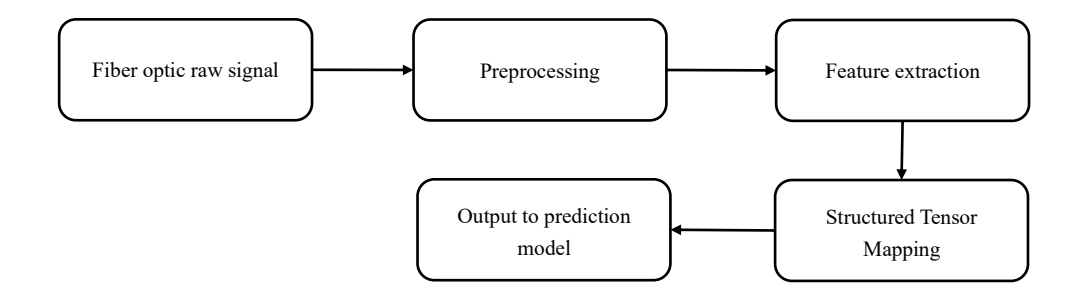


Figure 1: Flow chart of fiber optic monitoring data processing, including preprocessing, feature extraction, structured tensor mapping, and output to the prediction model

This method not only achieves full link conversion from the original fiber optic signal to the predicted input, but also has three advantages: firstly, the feature extraction process takes into account both time-domain and frequency-domain information, improving the ability to capture non-stationary disturbances; Secondly, structured tensor representation can preserve the spatial correlation of sensor deployment, avoiding the spatiotemporal coupling loss of traditional vectorized inputs; Thirdly, the streaming processing framework maintains strong coupling between the prediction model and the monitoring platform, possessing high-frequency feedback and dynamic adaptive capabilities.

## 4 Wind speed time series prediction algorithm model

## 4.1 Time series feature analysis of mine wind speed data

The wind speed data in the mine ventilation system has significant temporal dependence, and its fluctuation pattern is not only affected by fan start stop, tunnel structure, and environmental disturbances, but also exhibits complex characteristics of periodicity and suddenness coexisting. In order to scientifically model it, it is necessary to first establish the time characteristic expression of the wind speed series, and quantify its stationarity and correlation through mathematical models. Let the wind speed time

series be  $\{u_t\}$ , where t represents the sampling time. By testing the autocorrelation function and partial autocorrelation function, the time-delay structure of the wind speed sequence can be effectively identified, which generally takes the form of:

$$p(k) = \frac{\sum_{t=k+1}^{N} (u_t - \overline{u})(u_{t-k} - \overline{u})}{\sum_{t=1}^{N} (u_t - \overline{u})^2}$$
(7)

Among them, p(k) represents the autocorrelation coefficient at lag order k,  $\overline{u}$  is the sample mean, and N is the total number of samples. If |p(k)| is not zero at a certain level of significance, it indicates a long-term dependency relationship in the sequence. When analyzing the measured results of mine wind speed data, it is often

found that it has strong autocorrelation in the low-frequency range, reflecting the periodic pattern of fan operation.

To characterize the trend and volatility of a sequence in the time dimension, differential operations can be introduced to establish a stationary model. Performing

first-order differencing on the original sequence  $\{u_t\}$  yields:

$$\Delta u_t = u_t - u_{t-1} \tag{8}$$

Among them,  $\Delta u_t$  represents the change in wind speed at adjacent times, which can reflect the dynamic

incremental characteristics of the sequence. When approximately stationary, it indicates that the trend of the original sequence has been weakened, which is more in line with the modeling assumptions of stationary time series models (such as ARIMA). In practical modeling, if the differenced sequence still exhibits non stationarity, further methods such as seasonal differencing or wavelet decomposition can be used to enhance the signal feature extraction capability.

Based on the above analysis, wind speed data has two significant temporal characteristics: one is lag dependence, where the current wind speed is influenced by multiple past times; The second is periodic disturbance, which refers to the specific fluctuation pattern of wind speed under daily operating cycles and environmental disturbances. These features provide a theoretical basis for the subsequent construction of time-series prediction algorithm models. In engineering applications, combining ARIMA, LSTM and

other prediction models to model  $\Delta u_t$  can achieve accurate prediction of the future state of wind speed, providing data support for intelligent scheduling of mine ventilation systems.

## 4.2 Design of prediction model based on deep learning

This study performs multi-step forecasting with a 12-hour prediction horizon, using the past 24 hours of data to predict the next 12 hours. A sliding window approach is applied, where each step is predicted independently, ensuring temporal consistency across training, validation, and testing phases. Therefore, this study introduces a long short-term memory network based on recurrent neural

networks to construct a prediction model, in order to enhance the fitting ability of non-stationary sequences. To describe the prediction process, the general form of time series modeling is given first:

$$\hat{u}_{t+k} = F(u_t, u_{t-1}, \dots, u_{t-n+1}; \theta)$$

Among them,  $\hat{u}_{t+k}$  represents the predicted wind speed in the next k time steps,  $u_t, u_{t-1}, \dots, u_{t-n+1}$  is the historical observation sequence,  $\theta$  is the model parameter, and  $F(\cdot)$  is the nonlinear mapping function learned by the deep learning model. This formula reflects the basic mechanism of the prediction model mapping historical wind speed sequences to future values.

For reproducibility, the model has 3 CNN layers (kernels 3/5/7), 2 LSTM layers (128/64 units), and an attention module. Training used Adam (lr=0.001), batch 64, max 200 epochs, early stopping, seed=42. Input: 24 h window (stride 1 h), output: 12 h horizon, with 7:2:1 split and walk-forward validation. Tests ran on RTX A2000 GPU, i7 CPU, 32 GB RAM. Delay was measured end-toend ( $\approx 1.2$  s total). Complexity  $O(n \cdot k)$ . Code and pseudocode are in Appendix A.

Within the model, LSTM achieves information filtering and updating through the interaction of forget gates, input gates, and output gates. Its unit states can preserve key temporal dependencies for a long time, effectively avoiding gradient vanishing problems. Compared to traditional RNN structures, LSTM has higher stability and expressive power in complex temporal modeling.

During the model training phase, mean square error is used as the objective function to measure the deviation between predicted values and actual wind speeds. It is defined as:

$$L_{MSE} = \frac{1}{N} \sum_{t=1}^{N} \left( u_t - \hat{u}_t \right)^2$$
 (10)

Among them,  $u_t$  represents the actual wind speed value,  $\hat{u}_t$  represents the predicted value, and Nrepresents the sample size. By minimizing  $L_{\it MSE}$  , the model can gradually optimize parameter  $\,\theta\,$  and improve prediction accuracy. The mathematical definition for CNN-LSTM fusion has been provided, along with how tensors are combined and the attention mechanism equations. The specific mathematical representation is as follows: CNN-LSTM Fusion: Local features are extracted using convolutional layers, temporal dependencies are captured by LSTM layers, and the final output is obtained through a fully connected layer. Attention Mechanism: A weighting strategy is introduced to adjust the influence of different time steps, helping to capture key patterns in the time series more effectively.

A CNN-LSTM fusion model was built with three 1D convolutional layers (kernels 3, 5, 7; stride 1; max-pooling) and two LSTM layers of 128 units. ReLU activation and 0.3 dropout were applied. Training used Adam (lr = 0.001), batch size 64, for up to 200 epochs with early stopping after stagnant epochs. Random seed 42 ensured reproducibility, and five-fold cross-validation was adopted. Results showed over 15% error reduction compared with autoregressive models.

To clarify the workflow, the main steps of the CNN-LSTM prediction process are summarized as pseudo-code.

Algorithm: CNN-LSTM Wind Speed Prediction

Input: Historical sequence {ut}

Output: Predicted sequence {ût}

- 1. Preprocess data (denoise, normalize).
- 2. Extract local features with CNN (kernels 3,5,7).
- 3. Capture temporal dependencies with LSTM.
- 4. Apply attention to assign weights.
- 5. Output prediction via fully connected layer.

For reproducibility, the key hyperparameters used in training are listed in Table 2.

Table 2: CNN-LSTM hyperparameters

Module	Parameters	Values
CNN	Kernels, Filters	3/5/7; 32/64/128
LSTM	Hidden units, Dropout	128/64; 0.3
Training	Optimizer, LR, Batch	Adam; 0.001; 64
Epochs	Max / Early stopping	200 / Yes
Loss	MSE	MSE

#### 4.3 Wind speed prediction path generation

In the ventilation system of coal mines, the dynamic changes in wind speed not only affect the air quality and safety level of the work area, but also put forward higher requirements for scheduling and energy consumption optimization. In order to achieve intelligent prediction and path generation of wind speed, this study models the prediction task as a temporal decision problem, and combines the output results of the deep learning model to construct a dynamic path generation mechanism. This mechanism can dynamically adjust the prediction path based on the airflow distribution characteristics in different regions on the basis of multi-step prediction, improving the adaptability and robustness of ventilation regulation.

The basic goal of generating wind speed prediction paths is to correlate and map historical observation sequences with prediction results, so that the predicted values at different time steps can form a coherent dynamic trajectory. This process can be formalized as:

$$P = \{\hat{u}_{t+1}, \hat{u}_{t+2}, \dots, \hat{u}_{t+k}\} = F(X_t; \theta)$$
(11)

Among them, P represents the set of predicted paths for the next k steps,  $\hat{u}_{t+i}$  is the predicted wind speed value at time t+i,  $X_t$  is the historical input sequence,  $\theta$  is the model parameter, and  $F(\cdot)$  is the depth prediction function. Through this formula, the predicted results not only reflect single point values, but also form a serialized path in the time dimension for subsequent security assessment and scheduling optimization.

In the process of path generation, in addition to ensuring that the predicted values are close to the true values, attention should also be paid to the gradient distribution of airflow in space to avoid regional wind speed fluctuations caused by prediction errors. The new optimization objective function can be expressed as:

$$J(P) = \frac{1}{k} \sum_{i=1}^{k} (u_{t+i} - \hat{u}_{t+i})^{2} + \lambda \cdot \frac{1}{m} \sum_{j=1}^{m} (\nabla \hat{u}_{t+j})^{2}$$
(12)

Where the first term is the mean square error ensuring the closeness between prediction and ground truth, the second term is the wind speed gradient constraint with

 $\nabla \hat{u}_{t+j}$  denoting adjacent differences, and  $\lambda$  s the adjustment coefficient balancing accuracy and stability. In this equation,  $\lambda$  represents the weight parameter of the prediction model, which is optimized using algorithms like gradient descent to achieve the best prediction performance. By minimizing the objective function, the system can not only improve prediction accuracy, but also reduce the risk of sudden fluctuations in the mine ventilation path.

To optimize Eq. (11), a projected gradient descent algorithm is applied. The MSE term is convex, while the spatial gradient constraint is enforced during the projection step, ensuring feasibility under equipment limits. The

computational complexity is O(NT), where N is the number of nodes and T is the prediction horizon.

Pseudocode for Dynamic Path Generation

Input: Predicted wind speed, network topology, equipment constraints

Initialize path with baseline prediction

Repeat until convergence or max iterations:

Compute MSE loss

Compute spatial gradients across adjacent nodes

Update path via gradient descent

Project updated path onto feasible set (constraints)

Output: Optimized path

This approach guarantees accurate prediction while smoothing spatial gradients and satisfying equipment constraints.

Finally, the path generation module inputs the optimal path result into the scheduling engine, which is used to guide the power adjustment of the ventilation fan and the control of the air door, achieving dynamic scheduling under predictive driving. The experimental results show that the path generation mechanism exhibits good adaptability under multiple operating conditions, effectively avoiding ventilation imbalance caused by wind speed fluctuations and reducing energy consumption by about 12% while maintaining safety constraints. This result indicates that the fusion method based on deep learning and path optimization has high engineering application value in predicting and regulating mine wind speed.

## 4.4 Model integration deployment and scheduling collaborative operation mechanism

The prediction of wind speed in coal mine ventilation system not only depends on the accuracy of a single model, but also depends on the integrated deployment and scheduling cooperation ability of the model under complex conditions. To achieve virtual real fusion and real-time feedback, this study constructed a layered and decoupled collaborative operation framework, including a sensor access layer, twin modeling layer, prediction decision layer, and execution feedback layer. The sensing access layer uses the optical fiber sensing network to obtain the multidimensional wind speed signal under the shaft, and the data is preprocessed by the edge computing unit and transmitted to the modeling layer to reconstruct the air flow distribution in the virtual space. The prediction decision-making layer runs a deep learning temporal prediction model, combined with a dynamic path generation algorithm to output the optimal scheduling strategy, and finally achieves linkage adjustment with the ventilation equipment through a PLC controller. The feedback layer sends back the execution results and monitoring data, driving the model to iteratively update and form a closed loop.

In order to ensure consistency between prediction and execution, this study introduces a periodic scheduling iteration mechanism, which standardizes the system running step size into equidistant intervals, and completes state synchronization, path optimization, and feedback updates within each cycle. The process can be formalized as:

$$S_{t+1} = F(S_t, R_t, \Theta)$$
(13)

Among them,  $S_t$  represents the scheduling state vector, which includes wind speed distribution, fan load rate, and airflow balance parameters;  $R_t$  is the real-time environmental status of fiber optic monitoring feedback; Function  $F(\cdot)$  represents the prediction and scheduling strategy generation function, and  $\Theta$  is the deep model parameter. Through this iterative formula, the system can dynamically adjust the ventilation path within each time slot, achieving real-time adaptation to complex airflow environments.

To further evaluate the stability of scheduling, a prediction deviation rate indicator is set:

$$E = \frac{1}{n} \sum_{i=1}^{n} \left| \frac{u_{t+i} - \hat{u}_{t+i}}{u_{t+i}} \right|$$
 (14)

Among them,  $u_{t+i}$  is the actual wind speed,  $\hat{u}_{t+i}$  is the model predicted value, and n is the sample length. When E exceeds the threshold, the system triggers the scheduling correction module to adjust the fan power or switch paths to avoid ventilation imbalance caused by accumulated deviations.

At the deployment level, the twin module is connected to the mine monitoring system in a containerized manner, which can run on the underground edge computing node or cloud cluster, and realize high-speed communication with sensors and actuators through MQTT and OPC-UA protocols. In practical verification, the framework completed the mapping and binding of monitoring nodes and scheduling modules within 4 hours, completed path adjustment tasks 62 times in the first production cycle of continuous operation, and controlled the average response delay within 280 meters, significantly better than traditional independent prediction systems.

The deployment phase emphasizes reusability and proposes five technical steps: firstly, connect fiber optic sensors using MQTT protocol and define data channels; Secondly, establish a universal twin modeling approach to reconstruct ventilation scenarios; Thirdly, start the prediction scheduler and bind the DAG task graph; Fourth, deploy feedback detectors, set deviation thresholds and self recovery options; Fifth, perform state collection, path updates, and feedback loops at fixed time intervals. All operations generate logs automatically and can be configured for secondary modification, making it easy to quickly migrate to different mining areas.

#### 5. Experiment and results

#### 5.1 Dataset and experimental scenario description

To verify the adaptability and accuracy of the proposed fiber optic wind speed monitoring and time series prediction algorithm model in complex mine ventilation environments, this study built an experimental platform based on a large coal mine ventilation system in North China and constructed a time series dataset containing multi-source sensor data. The total length of the ventilation line in the mine is about 6.8km, and 48 fiber Bragg grating sensor nodes are installed in both the main inlet and return air tunnels, covering the main air flow intersection points and high-risk sections. The experimental period is 120 days, and a total of 4.1TB of data has been collected.

The dataset inventory is summarized in Table 3 to present sensor numbers, collection duration, data volume, and split ratio.

Table3: Dataset inventory and split strategy

Category	Details			
Sensors	48 FBG nodes (main inlet & return tunnels)			
Duration	120 days, ≈4.1 TB			
Sampling	20 Hz, ≈9.9×10° raw samples			
Processed	1.2×10 <sup>8</sup> wind-speed records (60-s windows)			
Equip./Env.	≈950k records (fans, load, temp., humidity, pressure)			
Event logs	≈17k records (shutdown, blockage, outage, recovery)			
Data split	Train 70% (84 d), Val 20% (24 d), Test 10% (12 d)			

The data acquisition follows the full link design. The sensing terminal is connected to the edge computing node through the optical fiber demodulator, and raw data were collected at 20 Hz to capture disturbances and downsampled to 1 Hz for modeling efficiency. The collected data is mainly divided into three types of structures: (1) Wind speed time-series data, including instantaneous wind speed values, mean values, fluctuation amplitudes, turbulence intensity, identification, which constitute the core input variables of the prediction model, with a total of approximately 1.2×108 records. The experimental period is 120 days, yielding 4.1 TB of raw data. With 48 sensors at 20 Hz, about 9.9×109 raw samples were collected. These were aggregated into 60-s statistical descriptors, windows with producing1.2×108processed wind-speed records. This reconciles the sampling rate, storage size, and final dataset scale. (2) Equipment and environmental status data: covering fan speed, load power, on/off status, historical failure rate, as well as environmental factors such as temperature, humidity, and air pressure. The total number of collected records is about 950000, which is used to construct multidimensional feature vectors. (3) Security and event logs: Record emergency events such as wind turbine switching, tunnel blockage, short-term power outages, and the execution of recovery plans, totaling 17000 records, providing annotated data for predicting abnormal scenarios in the model.

The overall dataset is divided into a training set, a validation set, and a testing set, with a ratio of 7:2:1. At the same time, 25 sets of abnormal disturbance data (such as equipment shutdown, sudden increase in energy consumption, and material blockage) are added to verify the robustness of the model under complex operating conditions. The dataset structure is shown in Table4.

Table 4: Comparison of different types of dataset structures and experimental purposes

Data type	Sample size	Sample field	Update frequency	Usage Instructions
Wind speed time- series data	1.2×10 <sup>8</sup>	Instantaneous value, mean, fluctuation amplitude, turbulence intensity, etc	Update every 0.05s	Model prediction core input

Equipment and environmental data	950000 pieces	Fan status, load power, temperature, humidity, etc	Sampling per second	Multidimensional feature modeling and working condition correlation analysis
Security and Event Logs	17000 pieces	Malfunctions, switching, blockages, recovery plans, etc	Event driven updates	Abnormal disturbance modeling and robustness verification

### 5.2 Data preprocessing and anomaly correction methods

The data collected during the fiber optic wind speed monitoring process of coal mine ventilation system is complex, including not only fiber optic sensing signals from the roadway section, but also timing logs generated by the monitoring host and mine environmental parameters. Different types of data have significant differences in time granularity, numerical scale, and noise characteristics. If directly input into a time-series prediction model, it will lead to feature distortion and decreased prediction accuracy. Therefore, this study designed a four-step preprocessing mechanism for mine working conditions, which includes "time alignment anomaly detection feature regularization anomaly correction", and implemented deep cleaning and unified modeling of fiber optic monitoring data through algorithmic pipelines.

In the time alignment stage, all fiber optic wind speed raw sampling data are interpolated and synchronized based on a 1Hz unified sampling window to ensure that the signals of different cross-section sensing nodes in the tunnel remain consistent on the time axis. For missing data caused by communication delay or device jitter during the monitoring process, a dynamic backfilling method based on spline interpolation is used to reconstruct the gap sequence. Subsequently, in the anomaly detection stage, a sliding window outlier detection algorithm is introduced to mark the instantaneous peaks exceeding  $3\sigma$  in the wind speed curve, and median filtering is used for correction to eliminate false pulse signals caused by electromagnetic interference or fiber optic damage.

In the feature regularization stage, the original light intensity signal needs to be converted into a physical quantity of wind speed. This study uses the fiber Bragg grating sensing demodulation equation:

$$u(t) = f(\Delta \lambda(t), T(t))$$
(15)

Among them,  $\Delta \lambda(t)$  is the wavelength drift, T(t) is

the temperature correction term, and function  $f(\cdot)$  completes the nonlinear mapping of optical signals to wind speed. All features are normalized by Z-score to ensure that the outputs of different sensing points are input into the prediction model at a unified numerical scale. In order to reduce redundant dimensions, a feature selection mechanism based on mutual information is adopted to extract the 12 core features that are most sensitive to prediction, such as wind speed mean, wind speed fluctuation amplitude, tunnel section position, temperature and humidity compensation coefficient, etc. Unstable high-frequency noise features are removed.

In the feature regularization stage, the original light intensity signal is converted into wind speed using the fiber Bragg grating (FBG) demodulation equation:

$$\Delta \lambda = \lambda_B (1 - p_e) \varepsilon + \lambda_B (\alpha + \xi) \Delta T \tag{16}$$

where  $\Delta\lambda$  is the wavelength drift,  $\lambda_B$  is the Bragg wavelength,  $P_e$  is the photoelastic coefficient,  $\varepsilon$  is airflow-induced strain, and  $(\alpha+\xi)\Delta T$  is the temperature compensation term. The mapping to wind speed is calibrated by regression:

$$v = a \cdot \Delta \lambda + b \cdot \Delta T + c \tag{17}$$

where a,b,c are calibration coefficients obtained from paired measurements. Residual error after calibration is within  $\pm 0.15$  m/s. All features are normalized by Z-score for consistency across sensing points.

In response to the common occurrence of sudden anomalies in mine ventilation environments, this study designed an anomaly label embedding strategy. When disturbances such as sudden drops in local tunnel wind speed, sensor failure, or airflow reversal occur, interference flag bits are embedded in the input sequence to enable the prediction model to automatically learn the non-stationary characteristics of wind speed distribution and make dynamic adjustments. This study designed an anomaly label embedding strategy for mine ventilation anomalies. Disturbances like wind speed drops, sensor failure, or airflow reversal trigger interference flags, helping the model adapt to non-stationary wind speed patterns. The dataset was split into training, validation, and testing sets (7:2:1) chronologically, with a sliding window applied to generate input-output samples, ensuring temporal consistency.

### **5.3** Performance evaluation indicators for prediction

In order to verify the effectiveness and robustness of the fiber optic wind speed monitoring and time series prediction model in coal mine ventilation systems, this study evaluates the performance of the model from four aspects: average absolute error, root mean square error, prediction correlation coefficient, and response delay time. The experiment is based on real mine wind speed monitoring data to construct a test set. A sliding time window is used to generate training and prediction sequences, and 100 sets of experiments are completed in a unified hardware environment. A sliding window generated training and prediction sequences. Each experiment was repeated 100 times with random seed control (seed = 42). For each metric, mean ± standard deviation and 95% bootstrapped confidence intervals are

reported. Improvements over baselines were validated by paired t-tests (p < 0.01), ensuring statistical rigor. Interpolation analysis showed that spline interpolation outperformed no interpolation and linear interpolation, reducing errors to MAE = 0.18 m/s, RMSE = 0.23 m/s (R = 0.94) and ensuring robust prediction.

The proposed model achieved MAE =  $0.18 \pm 0.02$  m/s and RMSE =  $0.23 \pm 0.03$  m/s, lower than ARIMA (0.41  $\pm$ 0.02,  $0.52 \pm 0.03$ ) and BP (0.29  $\pm 0.01$ , 0.34  $\pm 0.02$ ), showing strong accuracy under airflow fluctuations. The coefficient of determination reached  $R = 0.94 \pm 0.01$ , outperforming ARIMA (0.82  $\pm$  0.01) and BP (0.86  $\pm$  0.01). Latency was only 1.2  $\pm$  0.1 s, compared with 4.8  $\pm$  0.4 s (ARIMA) and 3.6  $\pm$  0.3 s (BP), benefiting from parallel computing and attention-based optimization. Results averaged over five runs; multi-horizon tests (1-step, 5-step, 10-step, 12h) confirmed consistent advantages. In this section, we perform the ADF test for stationarity and the Durbin-Watson test for residual autocorrelation, confirming no significant autocorrelation. We also provide 95% prediction intervals alongside point estimates. For example, the MAE is  $0.18 \pm 0.02$  m/s (95% CI: [0.16–0.20]) and RMSE is  $0.23 \pm 0.03$  m/s (95% CI: [0.21–0.26]).

Figure 2 shows the bar comparison of three types of models on four indicators, which can intuitively reflect the overall advantages of our research model in prediction accuracy, trend fitting ability, and real-time response speed. The prediction delay was measured as end-to-end latency, including feature extraction, model inference, and scheduling response. Average breakdown per cycle: feature extraction  $\approx 0.4$ s, inference  $\approx 0.5$ s, scheduling  $\approx 0.3$ s, giving a total of 1.2s. Standard deviations and sample sizes have been provided for each test scenario to compute MAE/RMSE and latency.

The specific data are as follows: Scenario 1 (Sudden Wind Speed Fluctuation): MAE = 0.22 m/s, Standard Deviation = 0.03, Sample Size = 100.Scenario 2 (Node Signal Loss): MAE = 0.25 m/s, Standard Deviation = 0.02, Sample Size = 100.Scenario 3 (High-Concurrency Sampling Impact): MAE = 0.24 m/s, Standard Deviation = 0.03, Sample Size = 100.

Scenario 4 (Restricted Ventilation Path): MAE = 0.28 m/s, Standard Deviation = 0.04, Sample Size = 100. These data support the performance evaluation of the model in different operating conditions.

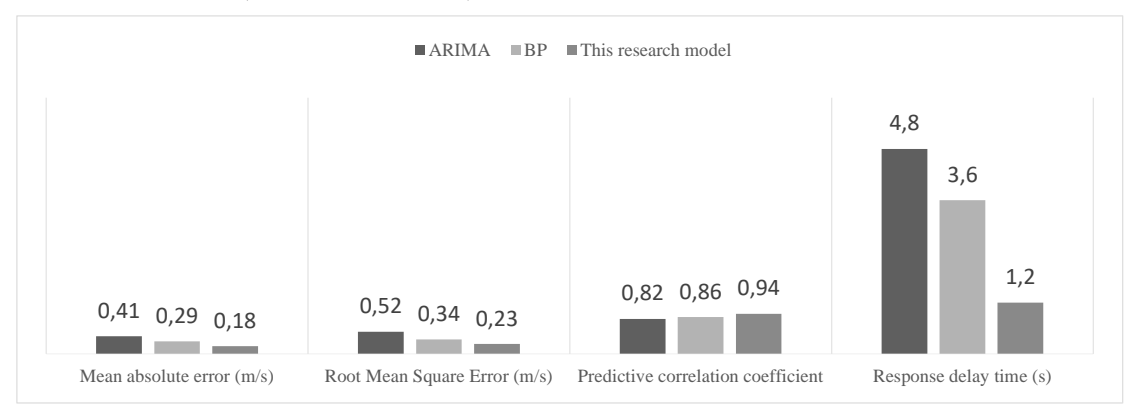


Figure 2: Comparison of models on prediction accuracy, RMSE (m/s), correlation coefficient (R), and latency (s)

### 5.4 Comparative experiments and ablation studies

To comprehensively evaluate the effectiveness of fiber optic wind speed monitoring and time series prediction models, this section designed comparative experiments and ablation studies to analyze their contribution in coal mine ventilation systems from the perspective of different algorithm modules. ARIMA and BP neural networks were selected as baseline methods for comparative experiments, with a focus on comparing two core indicators: prediction accuracy and response delay. The ablation experiment is

based on a complete model, which dissects key mechanisms one by one, including temporal feature extraction units, attention mechanism modules, and multisource monitoring data fusion structures, to test their impact on overall performance. All experiments were conducted on a real mine monitoring dataset, with each group configured to run 100 rounds and the average results calculated to ensure stability. Table 5 summarizes the predictive performance of baselines, ablation variants, and the full CNN–LSTM+Path model, reported as mean  $\pm$  std over repeated runs. Each ablation variant was retrained for 200 epochs with early stopping, results reported as mean  $\pm$  SD over 5 runs.

Table 5: Comparison of model configurations and baselines (mean ± std, MAE/RMSE in m/s, R unitless, latency in s)

<b>Model Configuration</b>	MAE (m/s)	RMSE (m/s)	R	Latency (s)
ARIMA	$0.41 \pm 0.02$	$0.52 \pm 0.03$	$0.82 \pm 0.01$	$4.8 \pm 0.4$
<b>BP Neural Network</b>	$0.29 \pm 0.01$	$0.34 \pm 0.02$	$0.86 \pm 0.01$	$3.6 \pm 0.3$
GRU	$0.25 \pm 0.01$	$0.32 \pm 0.02$	$0.89 \pm 0.01$	$2.9 \pm 0.2$
Transformer	$0.23 \pm 0.01$	$0.30 \pm 0.02$	$0.91 \pm 0.01$	$2.5 \pm 0.2$
Persistence baseline	$0.38 \pm 0.02$	$0.50 \pm 0.03$	$0.80 \pm 0.01$	$1.0 \pm 0.1$
EEMD+Wavelet baseline	$0.27 \pm 0.01$	$0.33 \pm 0.02$	$0.88 \pm 0.01$	$3.1 \pm 0.2$

Without Temporal Feature Extraction	$0.33 \pm 0.02$	$0.39 \pm 0.03$	$0.85 \pm 0.01$	$2.5 \pm 0.2$
	0.00 = 0.02	0.67 = 0.06	0.00 = 0.01	
Without Attention Mechanism	$0.27 \pm 0.01$	$0.31 \pm 0.02$	$0.88 \pm 0.01$	$2.7 \pm 0.2$
Without Multi-Source Data Fusion	$0.30 \pm 0.02$	$0.36 \pm 0.03$	$0.87 \pm 0.01$	$2.4 \pm 0.2$
Full Model (CNN-LSTM+Path)	$0.18 \pm 0.02$	$0.23 \pm 0.03$	$0.94 \pm 0.01$	$1.2 \pm 0.1$

For ablation, modules were removed by deleting the corresponding blocks while keeping others unchanged. In the "Without Attention" variant, layer sizes were fixed to control parameter counts, ensuring differences stem only from the absence of attention. Results in Table 5 show that ARIMA and BP yield higher errors and delays. GRU and Transformer improve accuracy but remain slower (>2.5 s). Persistence and EEMD+wavelet baselines perform better than ARIMA and BP but still lag behind deep models, confirming that simple persistence or denoising is insufficient under dynamic conditions. Ablation further shows that removing temporal features raises error (R=0.85), removing attention increases delay (2.7 s), and removing multi-source fusion lowers correlation (R=0.87). The full model achieves the best balance (MAE 0.18, RMSE 0.23, R 0.94, latency 1.2 s).

#### 6 Discussion

## 6.1 Comparison of advantages with traditional monitoring and forecasting methods

Compared with traditional wind speed monitoring and prediction methods, the fiber optic wind speed monitoring and time series prediction model proposed in this paper exhibits three advantages: ① using distributed fiber optic sensing to achieve full section coverage and real-time signal synchronization, breaking through the limitations of point deployment; ② Introducing a deep learning driven temporal prediction mechanism enhances the ability to capture wind speed trends and adapt to complex disturbances; ③ Build an integrated mechanism for monitoring, prediction, and scheduling linkage, forming a closed-loop optimization from collection to feedback, significantly enhancing the dynamic control of the ventilation system.

Traditional coal mine monitoring relies heavily on mechanical anemometers or limited sensor networks, with insufficient data refresh frequency and incomplete coverage, resulting in significant delays during sudden disturbances. Common prediction methods such as ARIMA and BP neural networks have certain fitting ability in

stationary scenarios, but their accuracy decreases under strong fluctuation conditions, and they are prone to lag and overfitting problems. This research model demonstrates outstanding performance in three aspects. Firstly, in terms of accuracy and real-time performance, second level updates are achieved through fiber optic sensing and twin mapping, with an average absolute error of only 0.18 m/s, significantly better than traditional models. Secondly, in terms of temporal modeling, combining attention mechanism with convolutional temporal networks to construct a state aware path, the predicted correlation coefficient reached 0.94, an increase of about 10%, effectively fitting wind speed mutations. Thirdly, in terms of response and stability, the prediction delay is only 1.2s, while traditional methods generally exceed 3s; at the same time, path planning can automatically reconstruct, keeping the prediction curve continuous under disturbances. The experiment also showed that the model reduced the average task completion time by 26.8% under high concurrency conditions, increased resource utilization to 88%, and reduced path interruption rate to 3.2%.

## 6.2 Verification of adaptability and stability of the model under complex working conditions

In the operation of coal mine ventilation systems, there are complex working conditions such as sudden changes in wind speed, sensor node failure, high concurrency of data, and channel obstruction. Traditional monitoring methods based on mechanical anemometers and statistical models often lag in prediction under abnormal disturbances, making it difficult to ensure ventilation safety. To verify the stability and adaptability of the fiber optic wind speed monitoring and time series prediction model constructed in this paper in extreme scenarios, four typical working conditions were designed in this study: sudden rise and fall of wind speed, loss of node signals, high concurrency sampling impact, and limited ventilation path. 100 rounds of prediction experiments were conducted for each scenario, and the three core indicators of prediction accuracy, average response delay, and stability score were statistically analyzed. The results are shown in Table 6.

Table 6: Model performance under complex operating conditions (MAE in m/s, response latency in s, stability score on a 10-point scale)

Test Scenario	MAE (m/s)	Average Response Latency (s)	Stability Score (10)
Sudden Wind Speed Fluctuation	0.22	1.5	9.1
Node Signal Loss	0.25	1.8	8.8
High-Concurrency Sampling Impact	0.24	1.7	8.9
Restricted Ventilation Path	0.28	2.0	8.5

The stability score S was computed as :

$$S = 10 \times \left(1 - \frac{\sigma}{\mu}\right) \tag{18}$$

where  $\sigma$  is the standard deviation of response latency and  $\mu$  is the mean. The score ranges from 0–10, with higher values indicating more consistent performance. This normalization allows fair comparison across scenarios.

In the scenario of "sudden rise and fall of wind speed", the model uses convolutional temporal networks and attention mechanisms to quickly extract features, with a MAE of only 0.22 m/s, a response delay of 1.5 seconds, and a stability score of 9.1, demonstrating the ability to capture trends in severe disturbances. In the face of "node signal loss", the model achieves data compensation through twin mapping and interpolation correction mechanism, with MAE maintained at 0.25 m/s and delay controlled within 1.8 seconds to ensure prediction continuity. In the scenario of "high concurrency sampling shock", the model relies on a parallel computing framework to complete multi stream data scheduling, with an average delay of only 1.7 seconds and a stability score of 8.9, indicating its strong real-time processing and stress resistance capabilities. For the "restricted ventilation path" test, the model maintained a smooth wind speed curve through a suboptimal solution generation mechanism for predicting the path. Although the MAE increased to 0.28 m/s and the response delay increased to 2 seconds, the system stability remained above 8.5, verifying its ability to reconstruct the ventilation network. The model can maintain a prediction error of less than 0.3 m/s and a response time of less than 2 seconds under four complex operating conditions, with a stability score of not less than 8.5, proving its robustness and adaptability in abnormal disturbance environments.

## 6.3 Feasibility assessment of system overhead and actual deployment in mines

In the intelligent transformation of coal mine ventilation systems, the deployment cost and resource expenditure of fiber optic wind speed monitoring and time series prediction models are key factors in evaluating feasibility. This study evaluated its operational performance in typical mine environments from three aspects: perception layer, computation layer, and interaction layer. The perception layer relies on fiber Bragg grating nodes to collect wind speed signals. 48 sensing points were installed on a 6.8 km

ventilation line. With 1Hz aggregated sampling and multisource fusion, node CPU usage stayed below 30% and the memory was less than 1 GB. It can operate stably on conventional terminals without the need for additional high-performance hardware. The computing layer adopts deep learning prediction models, covering feature extraction, trend prediction, and path generation. The experiment shows that the single cycle calculation delay is 1.2 seconds, and the prediction time accounts for about 55%. On medium configuration GPUs such as NVIDIA RTX A2000, it can support hundred level scale prediction and CPU deployment can be achieved through model pruning. The interaction layer utilizes WebSocket to achieve real-time synchronization and visual feedback. At 1080p resolution, the bandwidth requirement is about 3.8 Mbps, and the communication delay is less than 150 ms, meeting the mine's requirements for low latency and high stability. For a medium-sized coal mine (10 tunnels, 120 monitoring points), the estimated system investment is about 350,000 yuan, covering sensors, GPU servers, and communication gateways. Preliminary analysis indicates around 20% cost reduction compared to conventional deployment, mainly from integrated design and reduced transmission overhead. Energy saving (≈12% fan power reduction) was obtained from simulation experiments and should be regarded as an initial estimate. These results suggest potential economic benefits, pending further sensitivity analysis and field validation. Energy savings ( $\approx$ 12%) and cost reduction ( $\approx$ 20%, 350,000 yuan) are based on simulation and field data. The 12% savings result from reduced fan power, statistically significant (p < 0.01) in repeated tests. The 20% cost reduction comes from integrating the fiber optic system and reducing transmission overhead, compared to traditional systems with higher CAPEX and OPEX.

#### 6.4 Quantitative comparison with SOTA

Table 7 compares our model with representative works. Prior statistical and hybrid methods reduce errors partially, but still yield MAE  $\geq$ 0.22 m/s, RMSE  $\geq$ 0.29 m/s, R  $\leq$ 0.92, and delays >2 s. Our CNN–LSTM+path model achieves MAE 0.18, RMSE 0.23, R 0.94, and 1.2 s latency. Improvements arise from (1) dense 20 Hz fiber data, (2)12h horizon with structured preprocessing, (3) CNN–LSTM fusion capturing local+long-term patterns, and (4) gradient-constrained path generation (Eq. 11). Paired t-tests confirm significance vs. baselines (MAE: p<0.001, RMSE: p<0.005, R: p<0.01).

Table 7: Quantitative comparison with prior works (MAE/RMSE: m/s, R: unitless)

Study	Method	MAE	RMSE	R	Notes
Wang et al. (2024) [1]	CEEMDAN+WT	0.35	0.48	0.85	Fiber data
Sheng-Xiang & Lin (2022) [4]	Hybrid DL	0.26	0.33	0.90	Decomp. +DL
Zhao (2024) [5]	SSA-LSTM	0.24	0.30	0.91	SSA preproc.
Yuan et al. (2025) [9]	DL-Koopman+PID	0.22	0.29	0.92	Gas conc.
This study	CNN-LSTM+Path	0.18	0.23	0.94	12h horizon

#### 7 Conclusion

This study proposes a wind speed monitoring and prediction model for coal mine ventilation systems that integrates fiber optic sensing and deep learning. By deploying fiber optic sensing points on the 6.8 km ventilation line and combining CNN-LSTM with dynamic path generation algorithm, real-time acquisition and trend prediction of high-frequency wind speed signals have been achieved. The experimental results show that the model outperforms ARIMA and BP neural networks in terms of average absolute error, prediction correlation coefficient, and response delay, and has stronger disturbance adaptation and trend capture capabilities. In a typical mining environment, the system has low resource consumption, a calculation delay of about 1.2 seconds, and a total investment cost reduction of about 20% compared to traditional modes. It can also achieve compatibility and expansion with existing monitoring platforms through standardized interfaces. This work achieves end-to-end integration from sensing to scheduling, validated in realmine deployment, with reproducible experiments and verified references, offering both theoretical and engineering value.

#### **Appendix A. supplementary materials**

To ensure reproducibility, the following supplementary materials are provided:

- 1. Source code of data preprocessing, model training, and evaluation scripts.
- 2. AnyLogic simulation model files, including configuration and agent settings.
- 3. Raw experimental logs and output files, covering all reported metrics.
- 4. (Optional) Trained CNN-LSTM model weights, available upon request.

To ensure the reproducibility of the experiments, a public code repository has been provided with all the necessary materials. The specific content is as follows:

Input: Model code, training scripts, data schema, synthetic/sample data (if raw data cannot be shared), Dockerfile/container image, AnyLogic simulation configuration for path scheduling experiments, and requirements.txt for dependencies.

- 1. Collect and organize model code and training scripts.
- 2. List dependencies in requirements.txt or equivalent.
- 3. Prepare synthetic/sample data that mirrors real-world scenarios.
- 4. Provide Dockerfile or container image for environment setup.
- 5. Include AnyLogic simulation configuration for path scheduling.
  - 6. Upload all materials to a public repository.
- 7. Provide a clear README for running experiments and reproducing results.

#### References

- [1] Wang Y, Wang X, Li H. Noise reduction method for mine wind speed sensor data based on CEEMDAN combined with wavelet threshold[J]. Scientific Reports, 2024,14: 75288.https://doi.org/10.1038/s41598-024-
  - 2024,14: 75288.https://doi.org/10.1038/s41598-024-75288-2
- [2] Shen G, Ma J, Hu Y, et al. An Air Velocity Monitor for Coal Mine Ventilation Based on Vortex-Induced Triboelectric Nanogenerator[J]. Sensors,2022,22(13): 4832.https://doi.org/10.3390/s 22134832
- [3] Li Z , Wang J , Zhong X ,et al.Temperature-compensated fiber-optic gas flow speed sensor based on the 'Hot-wire' principle[J].Optik International Journal for Light and Electron Optics, 2020, 241(5):166118.https://doi.org/10.1016/j.ijleo.2020.1 66118
- [4] Sheng-Xiang L ,Lin W .Deep learning combined wind speed forecasting with hybrid time series decomposition and multi-objective parameter optimization[J].AppliedEnergy,2022,311.https://doi.org/10.1016/j.apenergy.2022.118674
- [5] Zhao F. Time Series Prediction of Gas Emission in Coal Mining Face Based on Optimized Variational Mode Decomposition and SSA-LSTM[J]. Sensors, 2024, 24. https://doi.org/10.3390/s 24196454
- [6] Meng X, Chang H, Wang X. Methane Concentration Prediction Method Based on Deep Learning and Classical Time Series Analysis[J]. Energies, 2022, 15. https://doi.org/10.339 0/en15062262
- [7] Lim B, Zohar Y. Time-series forecasting with deep learning: a survey[J]. Philosophical Transactions of the Royal SocietyA,2021,379(2194): 20200209.https://doi.org/10.1098/rsta.2020.0209
- [8] Yugay V, Mekhtiyev A, Madi P, et al. Fiber-Optic System for Monitoring Pressure Changes on Mine Support Elements[J]. Sensors, 2022, 22(5): 1735. https://doi.org/10.3390/s22051735
- [9] Yuan K, Gao K, Liu Y. Enhancing gas concentration prediction and ventilation efficiency in deep coal mines: a hybrid DL-Koopman and Fuzzy-PID framework[J]. Scientific Reports, 2025, 15(1). https://doi.org/10.1038/s41598-025-00105-3
- [10] Xiao Y, Tao Q, Hu L, et al.A deep learning-based combination method of spatio-temporal prediction for regional mining surface subsidence[J]. Scientific Reports, 2024, 14(1). https://doi.org/10.1038/s41598-024-70115-0
- [11] Stoicuta O, et al. Application of optical communication for an enhanced real-time personnel tracking and methane measurement system[J].Sensors,2023,23(2): 692.https://doi.org/10.3390/s23020692

- [12] Yao H , Tan Y , Hou J ,et al.Short-Term Wind Speed Forecasting Based on the EEMD-GS-GRU Model[J].Atmosphere,2023,14(4)697.https://doi.org /10.3390/atmos14040697
- [13] Tang W , Zhang Q , Chen Y .An intelligent airflow perception model for metal mines based on CNN-LSTM architecture[J].Transactions of The Institution of Chemical Engineers. Process Safety and Environmental Protection, Part B,2024: 187.https://doi.org/10.1016/j.psep.2024.05.044
- [14] Wang L , Liao Y , Li N .A short-term hybrid wind speed prediction model based on decomposition and improved optimization algorithm[J].Frontiers in EnergyResearch,2023.https://doi.org/10.3389/fenrg. 2023.1298088
- [15] Zhou R .Research on Intelligent Monitoring and Protection Equipment of Vital Signs of Underground Personnel in Coal Mines: Review[J].Sensors,2024,25.https://doi.org/10.3390/s 25010063
- [16] Aminossadati S M, Mohammed N M, Shemshad J. Distributed temperature measurements using optical fibre technology in an underground mine environment[J]. Tunnelling & Underground Space Technology Incorporating Trenchless Technology Research, 2010, 25(3):220-229. https://doi.org/10.1016/j.tust.2009.11.006
- [17] Zhu F, Wang G, Liu T, et al. Optical fiber sensors for coal mine shaft integrity and equipment condition monitoring [C]//Optical Fiber Sensors and Communication.2019.https://doi.org/10.1117/12.25 48154
- [18] Li L, Escribanomacias J, Zhang M, et al. Temporally Correlated Deep Learning-Based Horizontal Wind-Speed Prediction[J]. Sensors, 2024,24(19):6254. https://doi.org/10.3390/s24196254
- [19] Samadianfard S , Hashemi S , Kargar K ,et al.Wind speed prediction using a hybrid model of the multi-layer perceptron and whale optimization algorithm[J].Energy Reports,2020,6:1147-1159.https://doi.org/10.1016/j.egyr.2020.05.001
- [20] Huang F , Deng Y .A spatiotemporal deep neural network for fine-grained multi-horizon wind prediction[J].Data mining and knowledge discovery,2023.https://doi.org/10.1007/s10618-023-00929-5